Effect of expiratory flow limitation on respiratory mechanical impedance: a model study

R. PESLIN, R. FARRÉ, M. ROTGER, AND D. NAVAJAS

Laboratorio de Biofisica i Bioenginyeria, Facultat de Medicina, Universitat de Barcelona, Spain; and Unité 14 de Physiopathologie Respiratoire, Institut National de la Santé et de la Recherche Médicale, Université Henri Poincaré, 54511 Vandoeuvre-les-Nancy, France

Peslin, R., R. Farré, M. Rotger, and D. Navajas. Effect of expiratory flow limitation on respiratory mechanical impedance: a model study. *J. Appl. Physiol.* 81(6): 2399–2406, 1996.—Large phasic variations of respiratory mechanical impedance (Zrs) have been observed during induced expiratory flow limitation (EFL) (M. Vassiliou, R. Peslin, C. Saunier, and C. Duvivier. *Eur. Respir. J.* 9: 779–786, 1996). To clarify the meaning of Zrs during EFL, we have measured from 5 to 30 Hz the input impedance (Zin) of mechanical analogues of the respiratory system, including flow-limiting elements (FLE) made of easily collapsible rubber tubing. The pressures upstream (Pus) and downstream (Pds) from the FLE were controlled and systematically varied. Maximal flow ($\dot{V}$max) increased linearly with Pus, was close to the value predicted from wave-speed theory, and was obtained for Pus-Pds of 4–6 hPa. The real part of Zin started increasing abruptly with flow ($\dot{V}$) >85% $\dot{V}$max and either further increased or suddenly decreased in the vicinity of $\dot{V}$max. The imaginary part of Zin decreased markedly and suddenly above 95% $\dot{V}$max. Similar variations of Zin during EFL were seen with an analogue that mimicked the changes of airway transmural pressure during breathing. After pressure and $\dot{V}$ measurements upstream and downstream from the FLE were combined, the latter was analyzed in terms of a serial (Zs) and a shunt (Zp) compartment. Zs was consistent with a large resistance and inertance, and Zp with a mainly elastic element having an elastance close to that of the tube walls. We conclude that Zrs data during EFL mainly reflect the properties of the FLE.

respiratory mechanics; mechanical analogue; maximal expiratory flow; forced oscillations; airway wall elasticity

RESPIRATORY IMPEDANCE (Zrs) measurements by forced oscillations (3) are increasingly used to assess respiratory mechanics in physiological and clinical applications. Useful features of the method are that it does not require active cooperation from the patient and, contrary to spirometric investigations (7, 17), does not alter the bronchomotor tone (23). This makes the method particularly adequate for studying airway response to bronchomotor drugs (11, 14, 29, 31, 32). A recent and promising application is the study of respiratory mechanics during mechanical ventilation (18, 20), where other approaches are either invasive and/or require muscular relaxation and/or require special flow ($\dot{V}$) patterns.

Impedance measurements relate the amplitude and phase of small sinusoidal pressure swings applied to the respiratory system to those of the resulting $\dot{V}$ oscillations superimposed on the respiratory $\dot{V}$. The impedance and its frequency dependence are interpreted with the use of models that usually postulate that the respiratory system is linear. This is clearly the

exception rather than the rule in patients with severe airway obstruction, in which case the impedance, like any other mechanical parameter, will vary with the amplitude and pattern of breathing. Nonlinearity of the system may also be responsible for harmonic distortion and cross talk between frequencies when the pressure input is a combination of sine waves, unless the components of the signal meet a number of criteria (13, 25). An extreme case of nonlinearity which, to our knowledge, has not been much discussed so far in the context of forced-oscillation studies, is the occurrence of expiratory flow limitation (EFL) during the measurements. Yet EFL is not exceptional during spontaneous breathing in patients with severe airway obstruction (9, 10); it is still more likely to occur during bronchomotor challenge and is a common finding in patients mechanically ventilated for acute respiratory failure (6, 8, 27, 28). In the latter situation, large variations of Zrs during the respiratory cycle have been reported, with much lower values of the imaginary part (Im) of Zrs during the expiratory phase than during the inspiratory phase (20). These variations have been attributed to EFL, an interpretation supported by observations in mechanical analogues including a flow-limiting segment and in artificially ventilated rabbits during EFL induced by a negative expiratory pressure (30).

The aim of this study was to further clarify the meaning of impedance data obtained during and near EFL. For this, we measured the input impedance (Zin) of mechanical analogues of the respiratory system, including a collapsible airway segment during steady $\dot{V}$, for various combinations of the upstream and downstream pressures.[1] We also studied the impedance of an analogue that mimicked the changes of lung recoil pressure with lung volume (VL) and reproduced respiratory variations of airway transmural pressure. The study showed that impedance measurements during EFL provide very little information on the structures situated upstream from the collapsible airway segment; the latter behaves as a large impedance pathway, shunted by an elastic element that is responsible for variations of the real part (Re) of Zin in either direction and for a systematic decrease of Im(Zin).

---

[1] Two pressure sources were used in this model study: one to produce expiratory flow ($\dot{V}$), and the second, at the other end of the system, to measure the impedance by forced oscillations. In accordance with the literature on forced expiration, the terms "upstream" and "downstream" in the text always refer to the former pressure source.
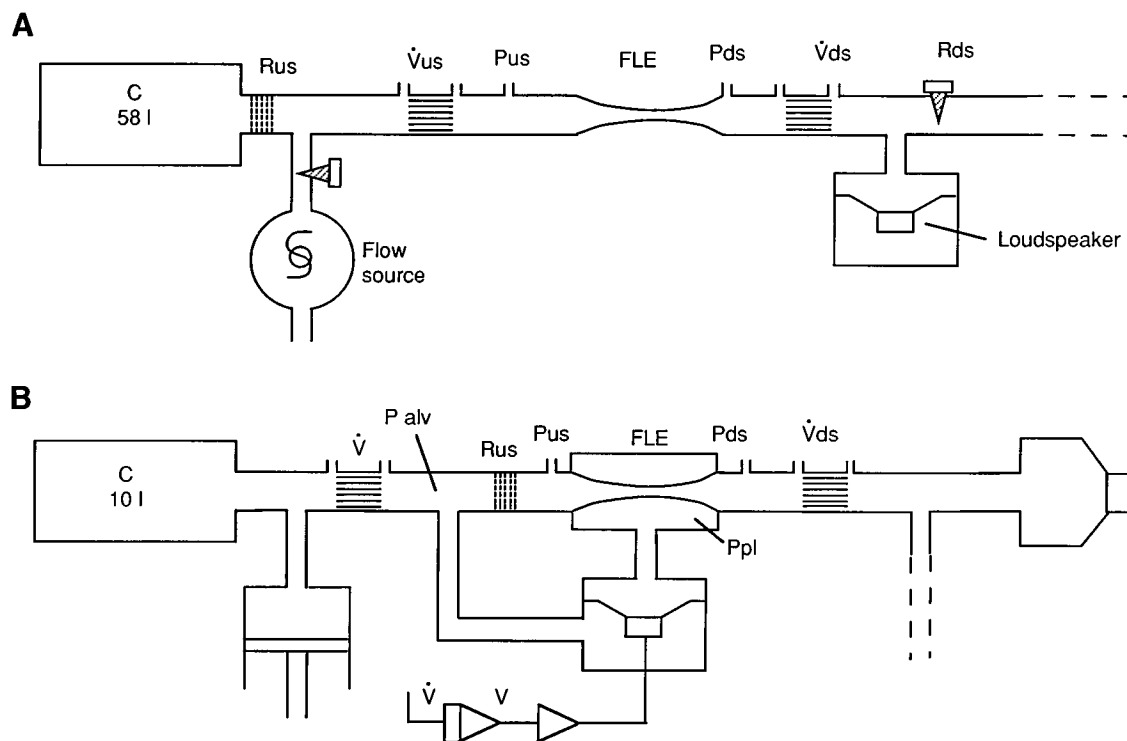
Fig. 1. *A*: experimental setup for constant-flow measurements. C, gas capacitance; Rus, upstream resistance; Rds, downstream resistance; FLE, flow-limiting element; Pus, Pds, $\dot{V}$us, $\dot{V}$ds, upstream and downstream pressures and flows, respectively. *B*: experimental setup to mimic changes of airway transmural pressure during breathing. $\dot{V}$, flow; V, volume; Palv, Ppl, alveolar and pleural pressures, respectively. See METHODS for explanations.

METHODS

Constant-flow measurements. The experimental setup used for constant-flow measurements is schematized in Fig. 1*A*. The mechanical analogue included a capacitive element made of a glass reservoir containing 58 liters of air (compliance of 41 ml/hPa for adiabatic compression) in series with a fixed resistor (Rus) and with a flow-limiting element (FLE). Rus was made of a variable number of layers of metal screen separated from each other by 1-mm intervals. It was linear within 5% up to $\dot{V}$ of 1 liter/s. The FLE was made of rubber tubing with a flat cross section (Burnet Distribution, Le Plessis-Robinson, France) that collapsed easily and had a virtually nil cross-sectional area at zero transmural pressure. The element was connected at both extremities to rigid tubes with a circular cross section, and the setup made it possible to vary its length so as to apply different strains and change its elastic properties. The tube used for most measurements (FLE A) had a thickness of 1 mm, a perimeter of 36 mm, and a resting length (L_0) of 110 mm. For some measurements, a similar but slightly thicker (1.2-mm) and wider (perimeter 41.2-mm) tube of the same length (FLE B) and a tube similar to FLE A except for its length (60 mm, FLE C) were used. The static pressure-volume (V) relationships of the tubes were measured by occluding one of their extremities and connecting the other to a syringe and high-impedance manometer (Honeywell 176PC/14); they were found to be approximately linear for distending pressures of 0–16 hPa. The corresponding elastances (Ew,st) for the two strains used in the study are given in Table 1, along with the axial Young moduli

$$Y = F/[A \cdot (\Delta L/L_0)] \tag{1}$$

(with *A* being the cross-sectional area of the tube walls) obtained by measuring their force-length (F-*L*) relationship.

A high-impedance $\dot{V}$ source, made of a powerful vacuum cleaner in series with a large resistance, was connected to the system between the fixed and the variable resistors and delivered a controlled $\dot{V}$ rate through the latter in the expiratory direction. The pressures upstream (Pus) and downstream (Pds) from the FLE were measured with similar piezoresistive transducers (Honeywell type 176PC/14), while the upstream flows ($\dot{V}$us) and downstream flows ($\dot{V}$ds) were sensed by Fleisch no. 2 pneumotachographs connected to differential pressure transducers (Celesco LCVR ±2 hPa). The four signals were low-pass filtered at 60 Hz (8 poles, Butterworth). The common mode rejection ratio (CMRR) of the $\dot{V}$ channels (21) was at least 60 dB at 30 Hz. The downstream end of the setup was connected to a tube and variable resistor (Rds) that were used to control the Pds, in parallel with a powerful loudspeaker (600 W; JBL type 800 Gti, 8-in. subwoofer) closed at the back to sustain the Pds. The loudspeaker was supplied with computer-generated sinu-

Table 1. *Characteristics of flow-limiting elements*

Characteristics	FLE A	FLE B	FLE C
Length, mm	110	110	60
Perimeter, mm	36.0	41.2	36.0
Thickness, mm	1.0	1.2	1.0
Ew,st, hPa/ml			
at $\Delta L/L_0 = 0.05$	4.0	4.2	12.1
at $\Delta L/L_0 = 0.10$	4.4		
Y, $10^6 \cdot$ N/m^2			
at $\Delta L/L_0 = 0.05$	1.31	1.51	
at $\Delta L/L_0 = 0.10$	1.50		

FLE, flow-limiting elements; Ew,st, static volumetric elastance of tube walls; Y, axial Young modulus; $\Delta L/L_0$, change in length/resting length.

soidal signals through a digital-to-analog conversion board (486-type PC equipped with Data Translation board 2801) and a power amplifier.

With FLE A at a strain of 0.05, measurements were performed at four levels of Pus (4, 8, 12, and 16 hPa) and, at each level, at a number of values of Pds. The latter was first made equal to Pus (infinite Rds, zero $\dot{V}$) and then decreased stepwise until a plateau of $\dot{V}$ was seen. The pressure outside the tube was always equal to barometric pressure, so that the $\dot{V}$ condition was entirely controlled by Pus and Pds. For each measurement, Pus and Pds were first set at the desired levels by varying the power supply of the $\dot{V}$ source, its serial resistance, and the variable resistor Rds. This required successive adjustments, because any change of Pds also modified Pus and vice versa. Then impedance measurements were performed successively at frequencies of 5, 10, 20, and 30 Hz. For this, the amplitude of the pressure oscillations was set at ~1 hPa peak to peak, and the pressure and $\dot{V}$ signals were sampled and digitized during 30 oscillation cycles at a rate of 32 points per cycle, using a second computer system and an all-purpose data-acquisition software (Labtech Notebook, Laboratory Technology, Wilmington, MA). Similar measurements were performed with FLE A at a strain of 0.10 and with FLE B and C at a Pus of 12 hPa and a strain of 0.05.

The dynamic characteristics of the FLE walls were also studied at the four oscillation frequencies and at distending pressures of 4, 8, 12, and 16 hPa. This was done by measuring the impedances of the FLEs with their upstream end occluded, using the Pds and transducers, the loudspeaker, and a pressure source in parallel with it.

Variable-flow measurements. A second setup was devised to mimic more closely the mechanical events during EFL (Fig. 1*B*) and, specifically, the changes in lung static recoil pressure (Pst,L) with VL. The "respiratory system" comprised, as previously, a gaseous capacitive element (compliance 7.1 ml/hPa), in series with a fixed resistor (Rus), the constant-flow source being replaced by a 3-liter syringe. The FLE was enclosed in a small chamber (380 ml) connected to one side of a box partitioned by a powerful loudspeaker (same as above); the pressure outside the FLE is analogous to pleural pressure (Ppl). The other side of the box was connected to a point situated upstream (or peripherally) from Rus, where the pressure is analogous to alveolar pressure (PA). Airway $\dot{V}$, measured close to the alveoli, was integrated analogically, providing a signal representing VL. The latter was passed through a power amplifier with an adjustable gain and sent to the just-mentioned loudspeaker; the latter therefore developed a pressure difference between the two sides of the box proportional to $\dot{V}$; this pressure difference represents PA − Ppl and is referred to thereafter as Pst,L. The sign of the signals was such that Pst,L increased (and Ppl decreased) when VL increased (inspiratory $\dot{V}$) and vice versa. To keep to the traditional phenomenological analysis of EFL (16, 24), the transmural airway pressure (Ptm) at the upstream end of our FLE varied with V and $\dot{V}$, in much the same way as it does in the lung

$$Ptm = Pst,L(V) + Rus \cdot \dot{V} \qquad (2)$$

Ptm increases during inspiration (increasing V and positive $\dot{V}$) and decreases during expiration (decreasing V and negative $\dot{V}$). With increasing expiratory effort, Ptm becomes negative, and $\dot{V}$ is limited in a volume-dependent manner. In our setup, the position and slope of the Pst,L(V) relationship could be modified at will by changing the volume at which the integrator was reset (Pst,L = 0) and the gain of the power amplifier, respectively. The relationship was quite linear over the volume range used in the study but exhibited some degree

of quasistatic hysteresis, which reflects the limitations of the loudspeaker as a pressure source at low frequencies.

The impedance of this device was studied with a type A FLE (strain 0.05) by recording the Pus and Pds and the $\dot{V}$us and $\dot{V}$ds with the same equipment as above. In addition, Ppl was recorded with a third piezoresistive transducer. By movement of the piston of the syringe manually, measurements were performed during ventilation with a tidal volume of ~1 liter and with various degrees of expiratory effort that permitted detection of EFL. The latter was accompanied by a very audible wheezing. Data were collected during periods of 20 s (sampling rate of 16 points per oscillation cycle), using different Pst,L(V) relationships and two values of Rus.

Data analysis. With the first setup, different impedances were computed from the recorded signals: *1*) the overall or input impedance of the system, $Zin = Pds/\dot{V}ds$; *2*) the impedance of the FLE itself, $Z_{FLE} = (Pds − Pus)/\dot{V}ds$; *3*) the impedance of that part of the system situated upstream from the FLE, $Zus = Pus/\dot{V}us$. With the second setup, only Zin and Z_{FLE} could be obtained because $\dot{V}$ was not measured immediately upstream from the FLE. In both instances, the $\dot{V}$ data were first corrected in the time domain for the time constants of the Fleisch pneumotachographs [2.1 ms (22)]. Then the Re and Im parts of the impedances were computed on a cycle-per-cycle basis from the Fourier coefficients of the signals. Next, the impedance data were corrected for the relative frequency responses of the corresponding transducers (assessed by applying simultaneously the same pressure input to the four transducers). Finally, the impedance data were averaged over the sampling period (first setup) or separately over the middle parts of the inspiratory and of the expiratory phases (second setup). The mean values of Pus, Pds, $\dot{V}$us, $\dot{V}$ds (and Ppl for the second setup) were also computed over the same periods.

RESULTS

Constant-flow measurements. The impedance of the walls of FLE A (Zw) with a strain of 0.05 at the four distending pressures is shown in Fig. 2. It behaved as an almost pure elastic element, with a negative reactance [Im(Zw)] varying hyperbolically with frequency and a negligible resistance (except at 5 Hz with the largest Ptm). The corresponding dynamic wall elastance (Ew,dyn; computed from the 5-Hz data) increased from 3.3 to 5.2 hPa/ml from the lowest to the highest Ptm, which is close to the value found in static conditions (Table 1). The data were almost the same with a strain of 0.10 (Ew,dyn from 3.6 to 5.3) and with FLE B (Ew,dyn of 4.3–4.6 hPa at a strain of 0.05), whereas the
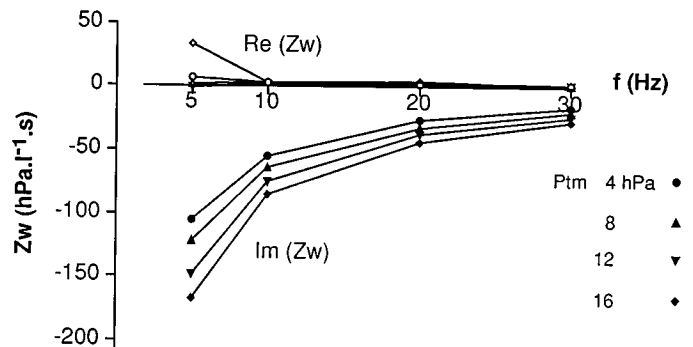

Fig. 2. Real (Re; open symbols) and imaginary (Im) parts of impedance (Zw) of the walls of FLE A at 4 transmural pressures (Ptm). f, Frequency.

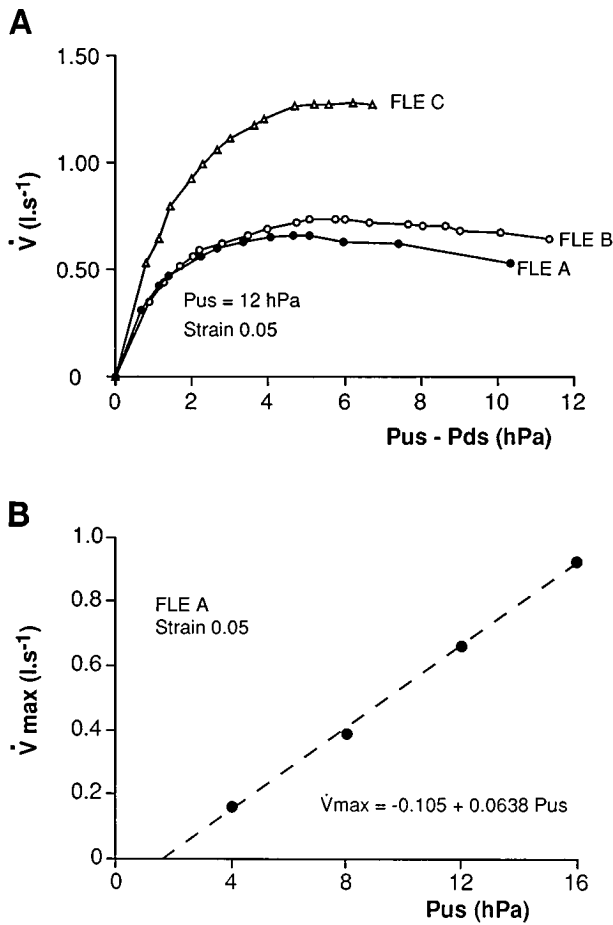**A**

B

Fig. 3. *A*: $\dot{V}$ through FLE as a function of difference between Pus and Pds. *B*: maximum flow ($\dot{V}$max) as a function of Pus with 1 of the FLEs.

shorter FLE was much stiffer (Ew,dyn of 6.7 to 8.1 hPa/ml). Zw also included a small resistive component that tended to decrease with increasing frequency and suggests that tube walls had some viscoelasticity.

The relationships between $\dot{V}$ and the driving pressure (Pus − Pds) of the three FLE at a Pus of 12 hPa and with a strain of 0.05 are shown in Fig. 3*A*. $\dot{V}$ reached a maximum $\dot{V}$max at driving pressures of 4–6 hPa. At higher pressures, the $\dot{V}$ decreased slightly but systematically and, at some point, the FLE started to flutter and emitted more and more noise with increasing pressure. $\dot{V}$max increased but slightly with increasing strain (0.70 at strain 0.10 with FLE A, compared with 0.66 at strain 0.05) and increased linearly with increasing Pus (Fig. 3*B*).

Impedance values obtained at the four frequencies with FLE A (strain 0.05) at a Pus of 12 hPa and with a value of Rus of 8.9 hPa·l^{-1}·s are shown in Fig. 4 for two $\dot{V}$ conditions. At 50% of $\dot{V}$max (Pus − Pds = 0.67 hPa), the resistance of the FLE [Re(Zfle)] represented ∼40% of the total [Re(Zin)] at all frequencies, whereas at $\dot{V}$max (Pus − Pds = 4.65 hPa) it represented almost all of it. In the latter condition, some of the pressure oscillations were transmitted upstream of the FLE (5–6%) but not enough to compute Zus with enough accuracy. Im(Zin) and Im(ZFLE), which were positive and increased with frequency at 50% $\dot{V}$max, became strongly negative at $\dot{V}$max, with a positive and irregular frequency dependence. The variations of Zin at 10 Hz as a function of the $\dot{V}$ for the three FLE (strain 0.05, Pus = 12 hPa, Rus = 8.9 hPa·l^{-1}·s) are further illustrated in Fig. 5. With all FLEs, Re(Zin) exhibited a slight positive $\dot{V}$ dependence up to ∼85% of $\dot{V}$max, then increased more abruptly with $\dot{V}$, and finally either further increased or suddenly decreased in the vicinity of $\dot{V}$max. Im(Zin) varied little up to 80–85% of $\dot{V}$max and decreased abruptly to become strongly negative above 95% of $\dot{V}$max. At driving pressures in excess of those necessary to achieve $\dot{V}$max, Im(Zin) remained strongly negative, which became usually also the case for Re(Zin). However, the data exhibited large fluctuations when the tube started fluttering. The changes

Fig. 4. Re and Im parts of input (Zin), upstream (Zus), and FLE (ZFLE) impedances at 50% of $\dot{V}$max and at $\dot{V}$max. FLE A, strain 0.05; Pus, 12 hPa; Rus, 8.9 hPa·l^{-1}·s.
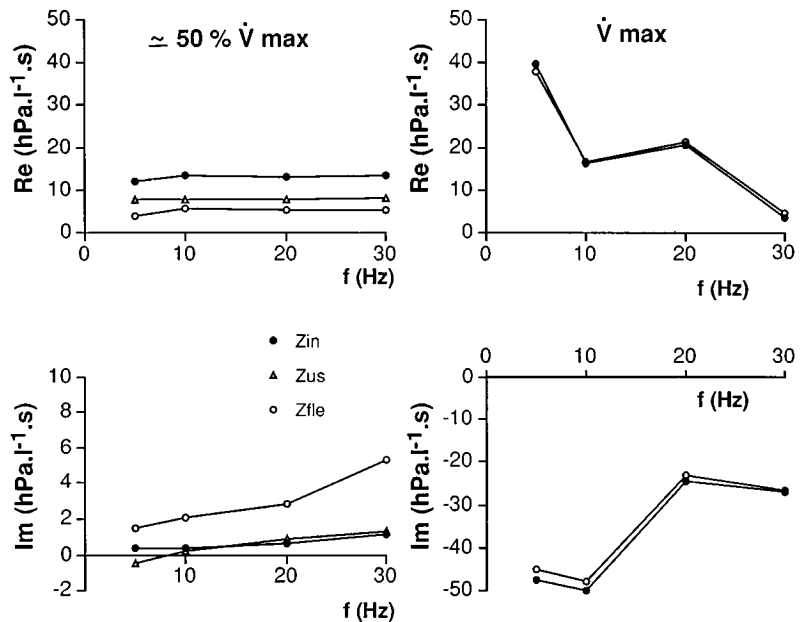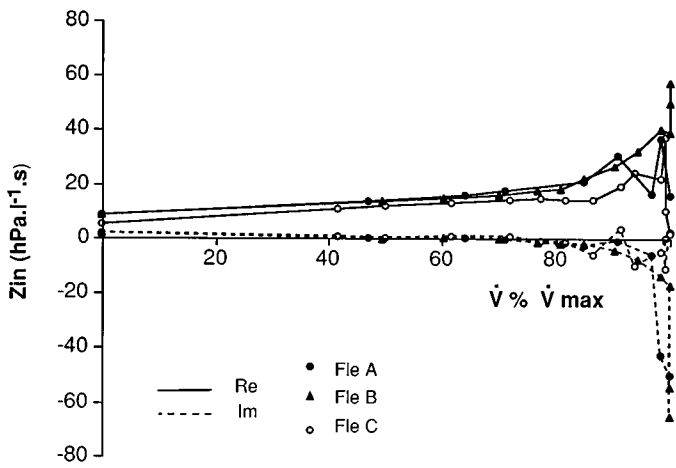
Fig. 5. Re and Im parts of Zin at 10 Hz as a function of $\dot{V}$ expressed as %$\dot{V}$max. Strain, 0.05; Pus, 12 hPa; Rus, 8.9 hPa·l^{-1}·s.

seen with FLE C were less dramatic than with the two longer FLE. Similar impedance profiles were observed at other Pus and with other values of Rus.

Variable-flow measurements. An example of the recordings obtained with the second setup is shown in Fig. 6. In that instance, Pst was ~2.5 hPa at end expiration and increased with V with a slope [static lung elastance (Est,L)] of 10.2 hPa/l; Ppl became positive during the expiratory phase. The V̇-V loops were very similar to those seen in humans during forced respiratory maneuvers. EFL is demonstrated by the fact that V̇ decreased while expiratory effort (Ppl) increased. Both Re(Zin) and Im(Zin) decreased suddenly during the expiratory phase at the time when the V̇ became limited. Mean values of Re(Zin) and Im(Zin)

during the middle part of the inspiratory and expiratory phases for two Pst,L(V) relationships and two values of Rus are shown in Fig. 7. In all instances and at all frequencies, Re(Zin) and Im(Zin) decreased markedly during the expiratory phase.

DISCUSSION

In agreement with our previous observations (20, 30), this study showed that V̇ limitation is responsible for large variations of the impedance measured by applying pressure oscillations downstream from a FLE. Specifically, Re(Zin) was seen to increase substantially above 85% of V̇max and then to vary sharply in either direction in the vicinity of V̇max. Changes in Im(Zin) were seen to start at larger V̇ (90–95% of V̇max) and to occur always in the same (negative) direction.

Before an attempt can be made to interpret these data, two points of methodology should be discussed. First, one should point out the practical difficulties of measuring with much accuracy as large impedances as found in this study. V̇ measurements with pneumotachographs require sensitive differential pressure transducers that, inevitably, have some dynamic asymmetry. The ones used in this study (Celesco LCVR) are among the best presently available (4), providing a CMRR slightly better than 60 dB at 30 Hz with short and optimally matched connecting tubes. Still, computer simulation and measurements on mechanical analogues (21) suggest that such a CMRR might be a little too low for accurately measuring the kind of impedance seen in this study. We do not believe, however, that this may have led to serious errors for two reasons. *1)* Impedances were only very large at the lowest fre-
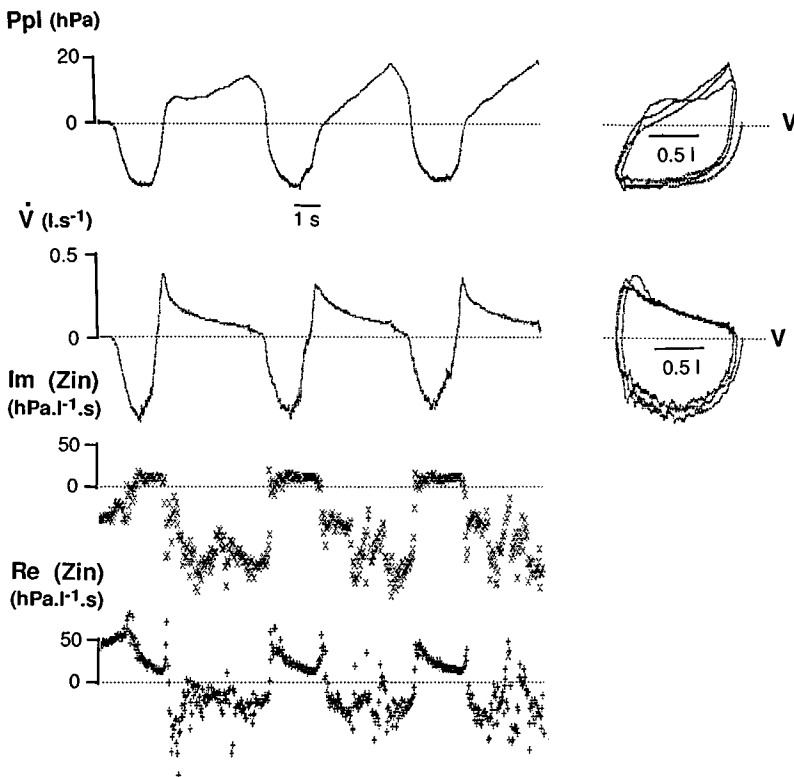

Fig. 6. Recording obtained during variable-flow measurements. *Top* to *bottom*: Ppl, V̇ (expiration up), Im and Re of Zin. *Right*: Ppl-V loops and V̇-V loops. Oscillation frequency, 30 Hz.

$Pst_0 = 2.2$ $Est,l = 15.2$ $Rus = 8.9$ $Pst_0 = 2.4$ $Est,l = 10.4$ $Rus = 8.9$
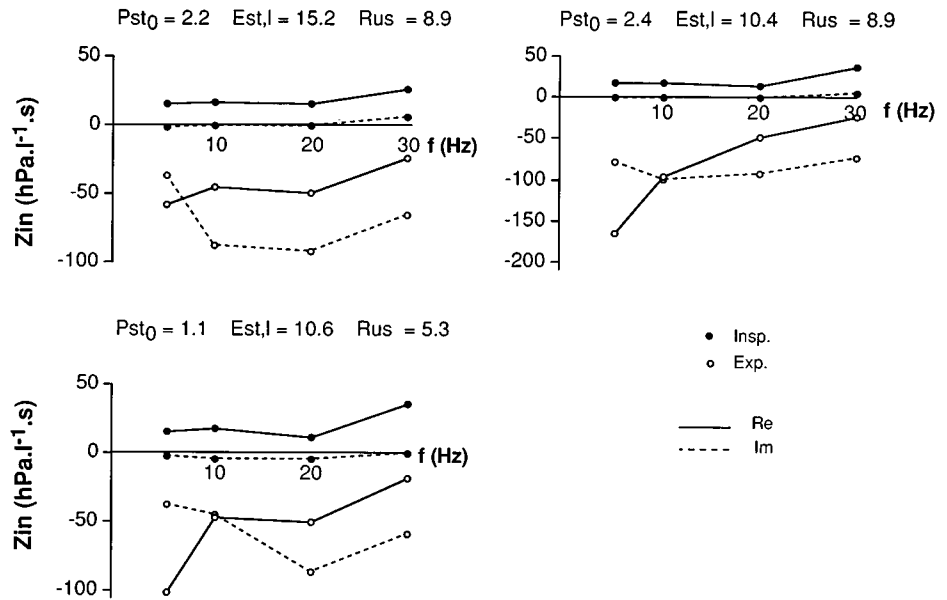
$Pst_0 = 1.1$ $Est,l = 10.6$ $Rus = 5.3$

Fig. 7. Re and Im parts of Zin during middle parts of inspiratory (Insp) and expiratory (Exp) phases with different values of upstream resistance (Rus, $hPa \cdot l^{-1} \cdot s$), static recoil pressure at end-expiration (Pst_0, hPa) and slopes of static pressure-volume relationship (Est,L, hPa/l).

- ● Insp.
- ○ Exp.
- —— Re
- - - - - Im

quency, where dynamic asymmetry is much less of a problem. *2*) No substantial changes in the values of Zw (Fig. 2) were seen when cross-exchanging the connections of the pneumotachograph to the two ports of the transducer, which is a reliable way to test the influence of this factor (21).

Second, the FLE used in this study were not meant to closely mimic human airways and actually differed from them in several respects. Wall elastance of FLE A and B were ~4 hPa/ml, whereas tracheal elastance derived from Ptm-V measurements is ~0.8 hPa/ml in adult humans (1), and total airway elastance has been estimated to 0.3 hPa/ml from the changes in anatomic deadspace with VL (15). Also, their F-L relationships had a much larger slope than observed in human tracheas [550 g for a 10% strain with FLE A, compared with ~20 g for adult tracheas (1)]. Thus, our tubes were much stiffer both radially and axially than human airways. On the other hand, the resting lumen of the tubes was almost zero, which, combined with the high elastance, resulted in very small cross-sectional areas. Because Vmax depends much more on the latter than on elastic properties of walls [$\dot{V}max = (1/\rho)^{1/2} \cdot (dPtm/dA)^{1/2} \cdot A^{3/2}$, where ρ is gas density (2)], the resulting Vmax was definitely lower than that seen in normal humans at the same Ptm. We have no reason to believe, however, that the behavior of our FLEs was

fundamentally different from that of human airways. Indeed, the impedance data were qualitatively similar with FLEs having different static elastances, and the observed Vmax values were close to those predicted from the above equation: 0.66 and 0.92 l/s for FLE A at Pus of 12 and 16 hPa, respectively, compared with 0.68 and 0.92 l/s computed from air density and A-Ptm relationship derived from static V-Ptm curve by dividing V by the length of the element. Moreover, Elliott and Dawson (5) observed that excised dog tracheas and rubber membrane artificial tracheas behaved similarly. Finally, the phasic variations of impedance seen with the second setup were very consistent with our previous observations in humans and in rabbits (20, 30).

Without entering into the complexities of fluid mechanics in collapsible tubes submitted to a mixed $\dot{V}$ input, which is beyond the scope of this study, our impedance data may tentatively be analyzed with a simple model (Fig. 8), where the FLE is represented by a shunt impedance (Zp) and a serial impedance (Zs). Zp accounts for the properties of the tube walls, lumped as a shunt pathway at the entrance of the tube, and Zs accounts for the resistive and inertial properties of the conduct itself. This model is in principle similar to that used by Mead (15) to describe the airways with their elastic wall. Zs and Zp may be obtained from the three
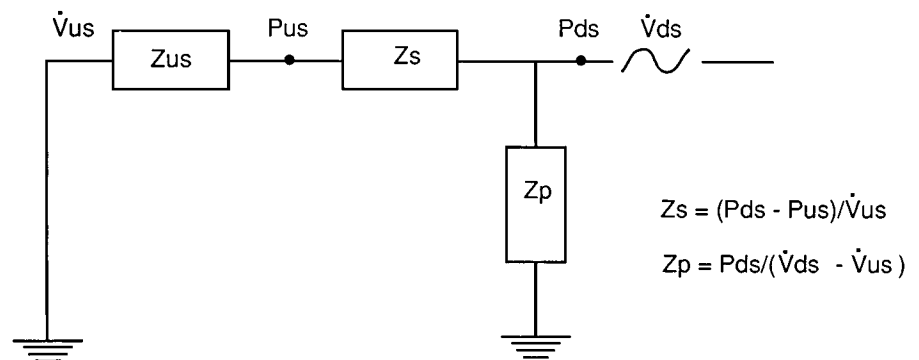
Fig. 8. Model used to analyze impedance data in terms of serial (Zs) and shunt (Zp) components of FLE.

$\dot{V}us$ Zus   Pus   Zs   Pds $\dot{V}ds$

Zp

$Zs = (Pds - Pus)/\dot{V}us$

$Zp = Pds/(\dot{V}ds - \dot{V}us)$

impedances measured with the first setup

$$Z_s = (P_{ds} - P_{us})/\dot{V}_{us} = Z_{FLE} \cdot Z_{us}/(Z_{in} - Z_{FLE}) \quad (3)$$

$$Z_p = P_{ds}/(\dot{V}_{ds} - \dot{V}_{us})$$

$$= Z_{in} \cdot Z_{us}/(Z_{us} + Z_{FLE} - Z_{in}) \quad (4)$$

The values of Z_s and Z_p computed from the impedance data obtained with FLE A (Pus, 12 hPa, strain 0.05; Rus, 8.9 hPa·l^{-1}·s) at 47, 85, and 97% of $\dot{V}$max are shown in Fig. 9. Values at $\dot{V}$max are not presented because $\dot{V}_{us}$ was too low to obtain reliable data. At all three $\dot{V}$ levels, Z_s is consistent with a resistance-inertance system, as expected for a tube, with a positive Re and a positive Im increasing almost linearly with frequency. The resistance and the inertance increase strongly with increasing $\dot{V}$, particularly in the vicinity of $\dot{V}$max, which may be interpreted as a lengthening and narrowing of the compressed segment of the FLE. On the other hand, Z_p is very similar to the impedance of the tube walls (Fig. 2); it is consistent with a mostly elastic system with little resistance (except at 97% $\dot{V}$max) and a negative Im varying hyperbolically with increasing frequency. Interestingly, Im varies little with $\dot{V}$ and corresponds to an elastance of ~4 hPa/ml, similar to that obtained on that FLE in static conditions (Table 1). Qualitatively similar data were obtained with a different strain and with a different value of Rus. Z_s and Z_p could not be computed from the data obtained with the second setup because $\dot{V}$ was not

Fig. 9. Re and Im parts of serial (Z_s, *top*) and shunt (Z_p, *bottom*) impedances of FLE A at 3 levels of $\dot{V}$ (%$\dot{V}$max); strain, 0.05; Pus, 12 hPa; Rus, 8.9 hPa·l^{-1}·s.

measured immediately upstream from the FLE. However, the values of Re(Zin) and Im(Zin) during the expiratory phases (Figs. 6 and 7) were of the same order of magnitude as those obtained with constant $\dot{V}$ at driving pressures in excess of those necessary to achieve $\dot{V}$max; it is therefore likely that the FLE behaved similarly during the simulated forced expirations as during constant $\dot{V}$ measurements. From this analysis, it appears that, close to $\dot{V}$ limitation, the FLE is equivalent to a high-impedance, resistive, and inertial pathway, shunted by an essentially elastic element, which almost completely masks the much lower upstream impedance.

An interesting and somewhat unexpected observation is that during $\dot{V}$ limitation some of the downstream pressure oscillations were still transmitted across the FLE. The upstream-to-downstream oscillation ratio increased with increasing values of Rus, reaching 8–10% with Rus = 17 hPa·l^{-1}·s. This observation is in agreement with the findings of Low et al. (12) but does not fit with the concept that a pressure disturbance cannot propagate upstream if the velocity of $\dot{V}$ is as fast as the pressure wave speed, which is the accepted physical explanation for the $\dot{V}$ limitation (2). Suki et al. (26), however, recently observed in excised calf tracheas that oscillatory pressure waves traveled substantially faster than the wave speed associated with $\dot{V}$ limitation. They suggested that it was related to differences in airway wall mechanics during small-amplitude oscillations and large-amplitude unidirectional wall motion. This could also explain why our FLEs did not behave as infinite impedances when $\dot{V}$ was limited. It may also be that the FLE acts as a half-wave rectifier, letting through the half of the oscillatory $\dot{V}$ wave that is below $\dot{V}$max and blocking the other half; however, as far as we can tell with the limited numerical resolution of our data, the small transmitted $\dot{V}$ and pressure waves were not clearly asymmetrical.

Another interesting observation is that the Re part of Zin became negative during constant-flow measurements when the driving pressure was above that necessary to achieve $\dot{V}$max. Such was also the case during most of the expiratory phase during variable-flow measurements (Fig. 6). This is surprising because input impedances of passive systems, contrary to transfer impedances, should always be positive. It suggests that some element in the system receives energy from another source than the forced oscillation generator, in this instance from the source of expiratory $\dot{V}$. Our tentative explanation is that, in the same way as they produce audible fluttering, large driving pressures amplify the vibrations of the tube walls induced by the forced oscillations; then the apparent resistance of the tube walls and, consequently, the Re part of Zin could be negative.

In practice, the observations made in this study indicate that input-impedance measurements during EFL provide very little information on the mechanical properties of the structures situated upstream from the FLE. In particular, close to $\dot{V}$max, the observed oscillatory resistance [Re(Zin)] may increase as well as decrease (Fig. 5) and may even be strongly negative (Figs. 6 and 7) when the driving pressure exceeds that
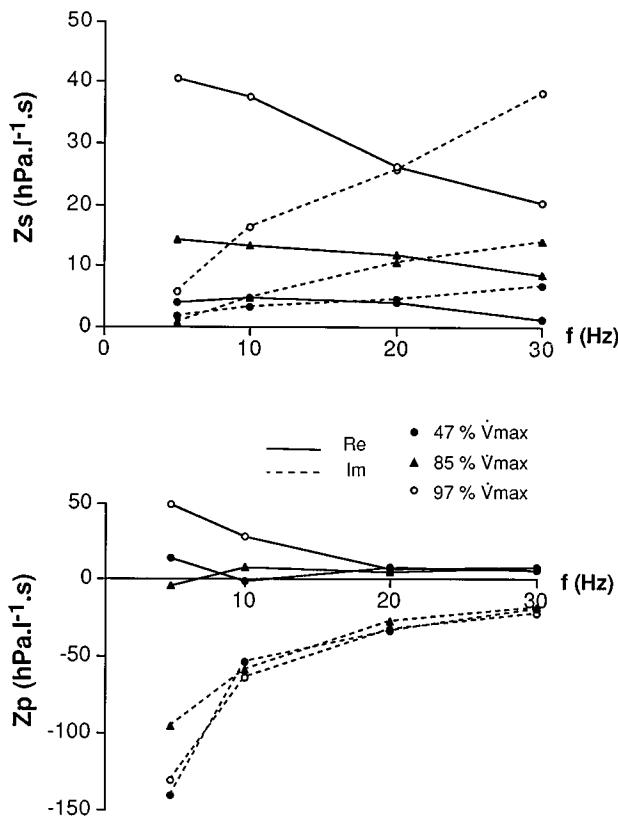
necessary to achieve V̇max. The average resistance over the respiratory cycle may, therefore, be extremely misleading in clinical applications. Similarly, nearing V̇max, Im(Zin) reflects less and less the properties of the upstream structures and more and more those of the tube walls which behave as a low-compliance pathway. The corresponding phasic changes in Im(Zin) during breathing are systematic enough to make a reliable sign of V̇ limitation. A practical conclusion is that, in all clinical or experimental situations where EFL could occur, impedance measurements should only be done by using input signals such that respiratory phasic variations may be easily detected and impedance separately computed for the inspiratory and expiratory phases. This precludes making measurements at low frequencies (for instance <5 Hz for usual breathing frequencies) and computing the impedance on data blocks exceeding half the breathing cycle. Separate measurement of expiratory and inspiratory impedances will permit both detection of EFL, which is undoubtedly the main mechanical abnormality of the patient, and assessment of respiratory mechanics when the airways are not compressed.

REFERENCES

1. **Croteau, J. R., and C. D. Cook.** Volume-pressure and length-tension measurements in human tracheal and bronchial segments. *J. Appl. Physiol.* 16: 170–172, 1961.

2. **Dawson, S. V., and E. A. Elliott.** Wave-speed limitation on expiratory flow: a unifying concept. *J. Appl. Physiol.* 43: 498–515, 1977.

3. **DuBois, A. B, A. W. Brody, D. H. Lewis, and D. F. Burgess.** Oscillation mechanics of lungs and chest in man. *J. Appl. Physiol.* 8: 587–594, 1956.

4. **Duvivier, C., M. Rotger, J. Felicio da Silva, R. Peslin, and D. Navajas.** Static and dynamic performances of variable reluctance and piezoresistive pressure transducers for forced oscillation measurements. *Eur. Respir. Rev.* 1: 146–150, 1991.

5. **Elliott, E. A., and S. V. Dawson.** Test of wave-speed theory of flow limitation in elastic tubes. *J. Appl. Physiol.* 43: 516–522, 1977.

6. **Gay, P. C., J. R. Rodarte, and R. D. Hubmayr.** The effects of positive expiratory pressure on isovolume flow and dynamic hyperinflation in patients receiving mechanical ventilation. *Am. Rev. Respir. Dis.* 139: 621–626, 1989.

7. **Gayrard, P., J. Orehek, C. Grimaud, and J. Charpin.** Bronchoconstrictor effects of a deep inspiration in patients with asthma. *Am. Rev. Respir. Dis.* 111: 433–439, 1975.

8. **Gottfried, S. B., A. Rossi, B. D. Higgs, P. M. A. Calverly, L. Zocchi, C. Bozic, and J. Milic-Emili.** Noninvasive determination of respiratory system mechanics during mechanical ventilation for acute respiratory failure. *Am. Rev. Respir. Dis.* 131: 414–420, 1985.

9. **Hage, R., J. G. J. V. Aerts, A. F. M. Verbraak, B. Van den Berg, and J. M. Bogaard.** Detection of flow limitation during tidal breathing by the interruptor technique. *Eur. Respir. J.* 8: 1910–1914, 1995.

10. **Kimball, W. R., D. E. Leith, and A. G. Robins.** Dynamic hyperinflation and ventilator dependence in chronic obstructive pulmonary disease. *Am. Rev. Respir. Dis.* 126: 991–995, 1982.

11. **Lebecque, P., S. Spier, J. G. Lapierre, Z. Lamarre, R. Zinman, A. L. Coates.** Histamine challenge test in children using forced oscillation to measure total respiratory resistance. *Chest* 92: 313–318, 1987.

12. **Low, H. T., Y. T. Chew, S. H. Winoto, and R. Chin.** Pressure/flow behavior in collapsible tube subjected to forced downstream pressure fluctuations. *Med. Biol. Eng. Comput.* 33: 545–550, 1995.

13. **Lutchen, K. R., K. Yang, D. W. Kaczka, and B. Suki.** Optimal ventilation waveforms for estimating low-frequency respiratory impedance. *J. Appl. Physiol.* 75: 478–488, 1993.

14. **Marchal, F., H. Mazurek, M. Habib, C. Duvivier, J. Derelle, and R. Peslin.** Input respiratory impedance to estimate airway hyperreactivity in children: standard method versus head generator. *Eur. Respir. J.* 7: 601–607, 1994.

15. **Mead, J.** Contribution of compliance of airways to frequency-dependent behavior of lungs. *J. Appl. Physiol.* 26: 670–673, 1969.

16. **Mead, J., J. M. Turner, P. T. Macklem, and J. B. Little.** Significance of the relationship between lung recoil and maximum expiratory flow. *J. Appl. Physiol.* 22: 95–108, 1967.

17. **Nadel, J. A., and D. F. Tierney.** Effect of a previous deep inspiration on airway resistance in man. *J. Appl. Physiol.* 16: 717–719, 1961.

18. **Navajas, D., R. Farré, M. Rotger, and A. Torres.** Monitoring respiratory impedance by forced oscillation in mechanically-ventilated patients. *Eur. Respir. Rev.* 4: 216–218, 1994.

19. **Pepe, P. E., and J. J. Marini.** Occult positive end-expiratory pressure in mechanically ventilated patients with airflow obstruction. *Am. Rev. Respir. Dis.* 126: 166–170, 1982.

20. **Peslin, R., J. Felicio da Silva, C. Duvivier, and F. Chabot.** Respiratory mechanics studied by forced oscillations during artificial ventilation. *Eur. Respir. J.* 6: 772–784, 1993.

21. **Peslin, R., P. Jardin, C. Duvivier, and P. Begin.** In-phase rejection requirements for measuring respiratory input impedance. *J. Appl. Physiol.* 56: 804–809, 1984.

22. **Peslin, R., J. Morinet-Lambert, and C. Duvivier.** Etude de la réponse en fréquence de pneumotachographes. *Bull. Physiopathol. Respir.* 8: 1363–1376, 1972.

23. **Peslin, R., C. Saunier, C. Gallina, and C. Duvivier.** Small-amplitude pressure oscillations do not modify respiratory mechanics in rabbits. *J. Appl. Physiol.* 76: 1011–1013, 1994.

24. **Pride, N. B., S. Permutt, R. L. Riley, and B. Bromberger-Barnea.** Determinants of maximum expiratory flow from the lungs. *J. Appl. Physiol.* 23: 646–662, 1967.

25. **Suki, B., and K. Lutchen.** Pseudorandom signals to estimate apparent transfer and coherence functions of non-linear systems: applications to respiratory mechanics. *IEEE Trans. Biomed. Eng.* 39: 1142–1151, 1992.

26. **Suki, B., O. F. Pedersen, R. H. Habib, and A. C. Jackson.** Wave speed during maximal expiratory flow and phase velocity from forced oscillations. *Respir. Physiol.* 102: 39–49, 1995.

27. **Valta, P., C. Corbeil, A. Lavoie, R. Campodonico, N. Koulouris, M. Chassé, J. Braidy, and J. Milic-Emili.** Detection of expiratory flow limitation during mechanical ventilation. *Am. J. Respir. Crit. Care Med.* 150: 1311–1317, 1994.

28. **Van den Berg, B., H. Stam, and J. M. Bogaard.** Effects of PEEP on respiratory mechanics in patients with COPD on mechanical ventilation. *Eur. Respir. J.* 4: 561–567, 1991.

29. **Van Noord, J. A., J. Clément, K. P. Van de Woestijne, and M. Demedts.** Total respiratory resistance and reactance as a measurement of response to bronchial challenge with histamine. *Am. Rev. Respir. Dis.* 143: 922–927, 1991.

30. **Vassiliou, M., R. Peslin, C. Saunier, and C. Duvivier.** Expiratory flow limitation during mechanical ventilation detected by the forced oscillation method. *Eur. Respir. J.* 9: 779–786, 1996.

31. **Wouters, E. F. M, A. C. Verschoof, A. H. Polko, and B. F. Visser.** Impedance measurements of the respiratory system before and after salbutamol in COPD patients. *Respir. Med.* 83: 309–313, 1989.

32. **Zerah, F., A. M. Lorino, H. Lorino, A. Harf, and E. Macquin-Mavier.** Forced oscillation technique vs spirometry to assess bronchodilatation in patients with asthma and COPD. *Chest* 108: 41–47, 1995.